A comparison between numerical predictions and experimental results for horizontal core-annular flow with a turbulent annulus

Ingen Housz, E.M.R.M.; Ooms, G.; Henkes, Ruud; Pourquie, MAthieu; Kidess, Anton; Radhakrishnan, R.

DOI
10.1016/j.ijmultiphaseflow.2017.01.020

Publication date
2017

Document Version
Accepted author manuscript

Published in
International Journal of Multiphase Flow

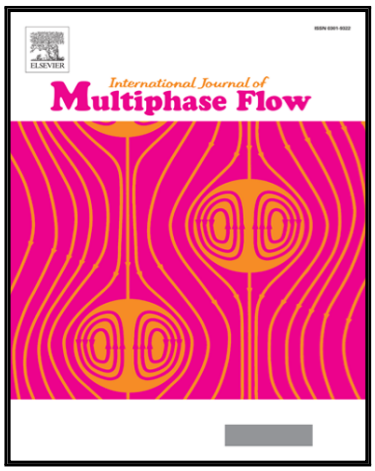

A comparison between numerical predictions and experimental results for core-annular flow with a turbulent annulus

E.M.R.M.Ingen Housz, G. Ooms, R.A.W.M. Henkes, M.J.B.M. Pourquie, A. Kidess, R. Radhakrishnan

PII: S0301-9322(16)30496-7
DOI: 10.1016/j.ijmultiphaseflow.2017.01.020
Reference: IJMF 2554

To appear in: *International Journal of Multiphase Flow*

Received date: 23 August 2016
Revised date: 9 December 2016
Accepted date: 23 January 2017

Please cite this article as: E.M.R.M.Ingen Housz, G. Ooms, R.A.W.M. Henkes, M.J.B.M. Pourquie, A. Kidess, R. Radhakrishnan, A comparison between numerical predictions and experimental results for core-annular flow with a turbulent annulus, *International Journal of Multiphase Flow* (2017), doi: 10.1016/j.ijmultiphaseflow.2017.01.020

HIGHLIGHTS

- Viscous oil experiments were done in horizontal core-annular flow with a turbulent water annulus.
- Numerical simulations were performed with a k-ϵ model at time-dependent, 3Dconditions.
- The simulations give a 15% lower pressure drop than the experiments.

A comparison between numerical predictions and experimental results for core-annular flow with a turbulent annulus

E.M.R.M. Ingen Housz,[1] G. Ooms,[1] R.A.W.M. Henkes,[1] M.J.B.M. Pourquie,[1] A. Kidess,[1] and R. Radhakrishnan[1]

J.M. Burgerscentrum, Delft University of Technology, Faculty of Mechanical Engineering, Laboratory for Aero- & Hydrodynamics, Mekelweg 2, 2628 CD Delft, The Netherlands

(Dated: 8 March 2017)

An experimental and numerical study has been made of oil-water core-annular flow in a horizontal pipe with special attention for the turbulence in the water. An experimental set-up was built to be able to compare numerical predictions with detailed experimental results. The oil density was considerably smaller than the water density. Full 3D and time-dependent numerical simulations of some of the experiments were done. Only when a turbulence model is applied the agreement with the experiments is reasonably good.

Keywords: Horizontal core-annular flow, turbulent annulus, numerical simulation, volume-of-fluid method. Topical heading: Transport Phenomena and Fluid Mechanics.

INTRODUCTION

We study the flow of a high-viscosity liquid surrounded by a low viscosity liquid through a horizontal pipe. Much attention has been paid in the literature to this core-annular flow. Joseph and Renardy[14] have written a book about it. There are several review articles, see for instance Oliemans and Ooms[24] and Joseph et al.[15]. An early publication was by Charles et al.[8]. Studies were published about the stability of core-annular flow and about the transition to other types of flow pattern (see for instance, Joseph and Renardy[14], Brauner and Maron[7], Rodriguez and Bannwart[30], Strazza et al.[32], Colombo et al.[9] and Sotgia et al.[31]). Other publications deal with the pressure drop over the pipe and the hold-up (see e.g. Oliemans et al.[25], Bai et al.[2], Arney et al.[1], Ullmann and Brauner[34], Bannwart[4], Strazza et al.[32], and Sotgia et al.[31]). Many studies deal with the development of waves at the interface between the high-viscosity liquid and the low-viscosity one (see Ooms[26], Bai et al.[2], Miesen et al.[23], Bai et al.[3], Renardy[28], Li and Renardy[22], Kouris and Tsamopoulos[19], Hung et al.[12], Ko et al.[18], Sotgia et al.[31] and Rodriguez and Bannwart[29]).

In an earlier publication (see Beerens et al.[5]) we made a comparison between numerical predictions and experimental results for laminar core-annular flow. In that publication we announced: "The numerical simulation of core-annular flow with a turbulent annulus and a wavy interface using the volume-of-fluid method in combination with a turbulence model is the next step in our research." In the present publication we will give a follow-up to this promise. We built an experimental set-up, in which experiments with a very viscous oil and water were carried out in a horizontal pipe. We knew, of course, that several core-annular-flow loops have been constructed by other researchers (see the literature survey given above). However, we wanted to be able to make a comparison between our numerical predictions and own detailed experimental results. Moreover carrying out experiments gives much insight in the flow pattern. The oil density was considerably smaller than the water density. The operating conditions were chosen to be such, that the flow was close to the transition between core-annular flow and stratified flow. This was achieved by reducing the mixture velocity and/or reducing the water addition ratio. The buoyancy force on the core (due to the density difference between the oil and water) caused the eccentricity of the oil core to be large and hence the water layer at the bottom to be rather thick. Therefore the

flow of water in the annulus at the bottom of the pipe was turbulent. We checked this by injecting a dye and confirmed that indeed the water flow is turbulent at that location. Special attention was given to measuring the increase of the pressure drop at these conditions as a function of the oil and water flow rates. The wave shape was determined with the aid of flow visualization with a high-speed camera.

As mentioned the emphasis of our study is on the possibility of simulating core-annular flow with turbulence in the water annulus. To that purpose some of the experiments were compared with their full 3D and time-dependent numerical simulation using the volume-of fluid method. Both the eccentricity of the core and the development of waves at the interface were taken into account. The simulations were carried out without and with a turbulence model. We applied the low-Re Launder-Sharma model. The simulation results and their comparison with the experiments are presented in this paper.

In the literature attention has been paid to the modelling of turbulent core-annular flow. A first approach was made by Oliemans (see for instance Oliemans et al. et al.[25]). They assumed the core to be solid and eccentric with waves at the core-annular interface. There thus was no deformation of the interface. The turbulence in the annulus was modelled by means of the mixing length model using the Van Driest hypothesis. Huang et al.[12] used a standard $k-\varepsilon$ model to study eccentric core-annularflow with a smooth interface. So the development of waves was not taken into account. Ko et al.[18] used the SST $k-\omega$ model for concentric core-annular flow with the development of waves at the interface. So in their work the influence of eccentricity was not included. Ghosh et al. performed[10] a CFD study to simulate turbulent core-annular flow through a vertical pipe. Also Kim and Choi[17] investgated turbulent core-annular flow in a vertical pipe. Jiang et al.[13] simulated turbulent core-annular flow through a II bend. Kraushik et al.[16] simulated turbulent core-annular flow through a sudden contraction and expansion.

I. EXPERIMENTS

A. Experimental set-up

In figures 1 and 2 schematic overviews of the front side and back side of the experimental set-up are shown. The measurements were carried out in a straight section of the PVC pipe loop, which has a diameter of 21 mm. The diameter is constant through the loop. The total length of the pipe loop is about 7.5 m and consists of different parts connected to each other with re-attachable links. These pipe sections are, in downstream order: a 2 m straight section, a bend with a radius of 0.25 m, a 3 m straight section (the measurement pipe), another bend with a radius of 0.25 m and a straight section of 0.5 m. There is a divider at the inlet to the pipe loop, which generates the core-annular flow. The divider has an inner pipe which is concentrically placed within an outer pipe. Oil is entering into the pipe loop via the inner pipe and water via the annular space between the two pipes. The oil pump and water flow rate meter were calibrated to enable measuring the oil and water flow rates. An inverted U-tube manometer was connected to two points of the measurement pipe to determine the pressure gradient. The pressure points were at the bottom of the pipe with the rather thick water layer, in order to reduce their fouling by the oil as much as possible. The experiments were repeated several times to check their reproducibility. The spreading in each of the pressure measurements was smaller than 5%. Flow visualization was obtained with a high-speed camera at a rate of 500 fps. A transparent box filled with water was built around the measurement pipe to improve the quality of the recordings. This removed distorsions from the pipe wall and it also helped to focus the camera at the top and bottom parts of the pipe, where the most interesting flow aspects of core-annular flow occur. The (Newtonian) oil used for the experiments was Shell Morlina S4 B 680. During an experiment the oil temperature was constant. Experiments were done at several temperatures between 19 ^{0}C and 21 ^{0}C. In this temperature range the viscosity is between 2700 cSt and 2300 cSt. The viscosity is strongly dependent on the temperature and it decreases with increasing temperature. The oil density is equal to 857 kg/m^3. Due to the relatively large density difference between the water and the oil there is a strong buoyancy force on the core and its eccentricity is large. This is important for this study, as the emphasis is on the occurence of the turbulence in the bottom part of the pipe flow.

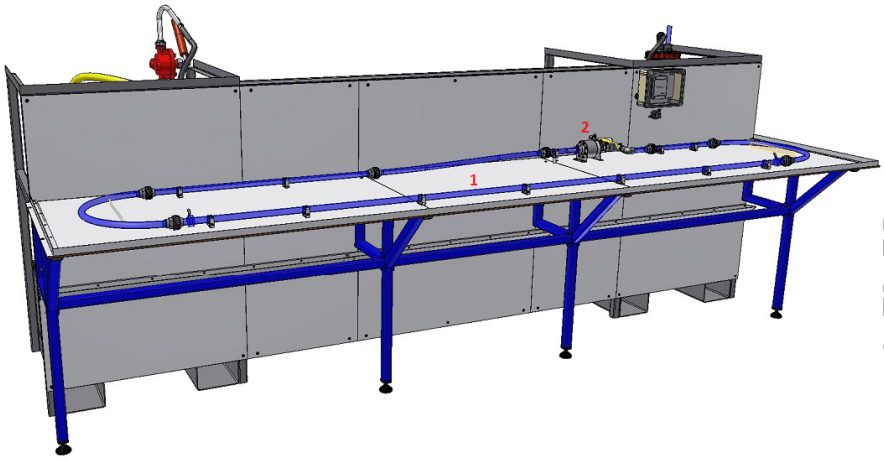

FIG. 1. Schematic overview of the front side of the experimental set-up

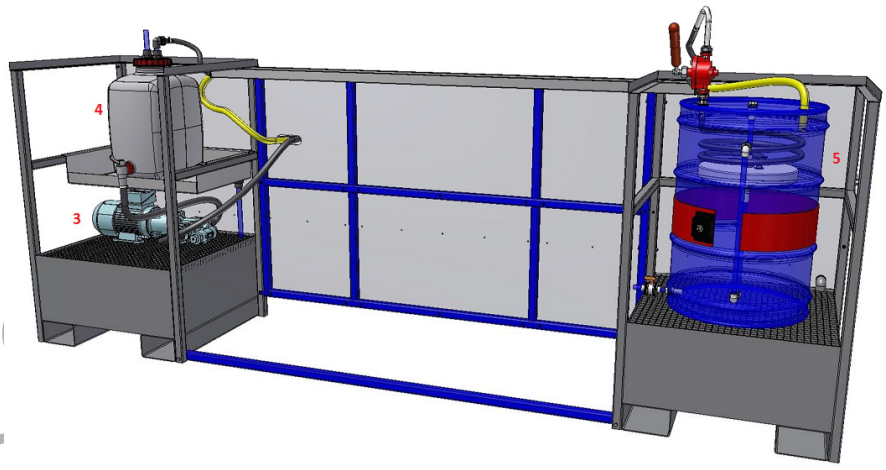

FIG. 2. Schematic overview of the back side of the experimental set-up

B. Experimental results

The experiments were performed at a certain value of the oil flow rate Q_0, during which the water flow rate was decreased (starting from a relatively large volumetric water addition ratio ϵ_w). The water addition ratio (or watercut) is defined as the ratio of the water flow rate and the total flow rate (water plus oil). These experiments were carried out at several values of the oil flow rate. Pictures of some experiments are shown in figure 3 and figure 4 for an oil flow rate of 0.28 l/s and a water percentage of 20% and 5% repectively. It can

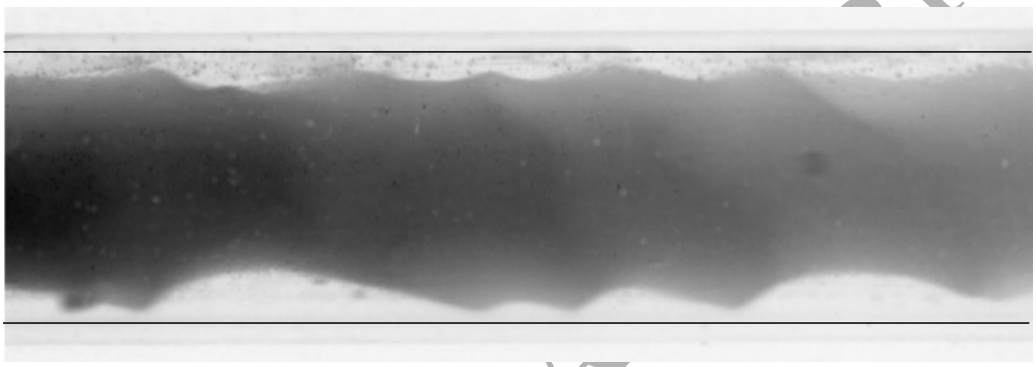

FIG. 3. Core-annular flow at an oil flow rate of $0.28\,l/s$ and a water addition ratio of $\varepsilon_w = 20\%$. The solid lines indicate the pipe wall.

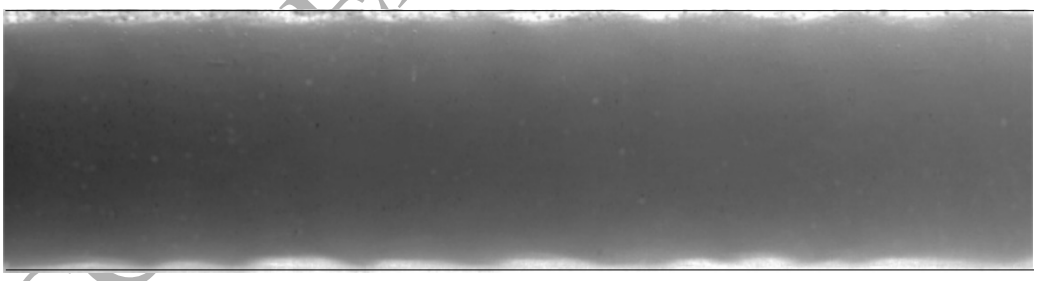

FIG. 4. Core-annular flow at an oil flow rate of $0.28\,l/s$ and a water addition ratio of $\varepsilon_w = 5\%$. The solid lines indicate the pipe wall.

be seen that at a large water addition ratio of 20 % the core is already very eccentric due to the buoyancy force on the core caused by the large density difference between water and oil. With a decreasing water addition ratio the thickness of the water film at the bottom of the pipe decreases strongly. The thickness of the water layer at the top decreases only slightly,

and the waves remain present. When the water addition ratio becomes too small, the core touches and fouls the pipe wall at the top and the core-annular flow pattern transfers into a stratified flow pattern.

The pressure drop Δp_m over the pipe, as measured during the experiments, is given in figure 5 for multiple oil flow rates. In the figure also the temperature is given, at which each oil flow rate was measured. As explained earlier temperature differences cause differences in the oil viscosity. A number of observations can be made from figure 5. Firstly the figure shows that (when starting at a large water addition ratio and decreasing its value), the pressure drop first decreases, reaches a minimum and then increases again. At a too small water addition ratio core-annular flow cannot exist anymore and the pressure drop increases strongly due to the fouling of the pipe wall at the top of the pipe. Secondly it can be concluded from the two cases for $Q_0 = 0.41\,\mathrm{l/s}$ at different temperatures, that the pressure drop is larger at the higher temperature (i.e. at the lower oil viscosity). Only close to the minimum in the curve the values of the pressure drop for the two temperatures are about the same.

As mentioned the emphasis of the study is on the influence of turbulence in the water annulus on core-annular flow. First we make a rough estimate of the Reynolds number of the water flow at the bottom part of the pipe. From the experiments we know that the water velocity is of the order $1.3\,m/s$. The thickness of the water layer is about $0.006\,m$, dependent on the water addition ratio used. This means that the Reynolds number is of the order $5.000 - 10.000$. There are waves present at the core-annular interface that disturb the flow. To find out whether the water layer at the pipe bottom was turbulent we injected dye into the water flow and observed the dye dispersion process. We noticed that the dye dispersed quickly into the water, showing the presence of turbulence in that region. (When we injected dye in a laminar pipe flow of water only, that was not the case.) An example is given in figure 6. To clearly see the dispersion process we have selected for this figure a water addition of 30 % and an oil/water mixture velocity of $0.7\,m/s$. However at smaller water percentages and larger mixture velocities turbulent spreading of the dye was always observed.

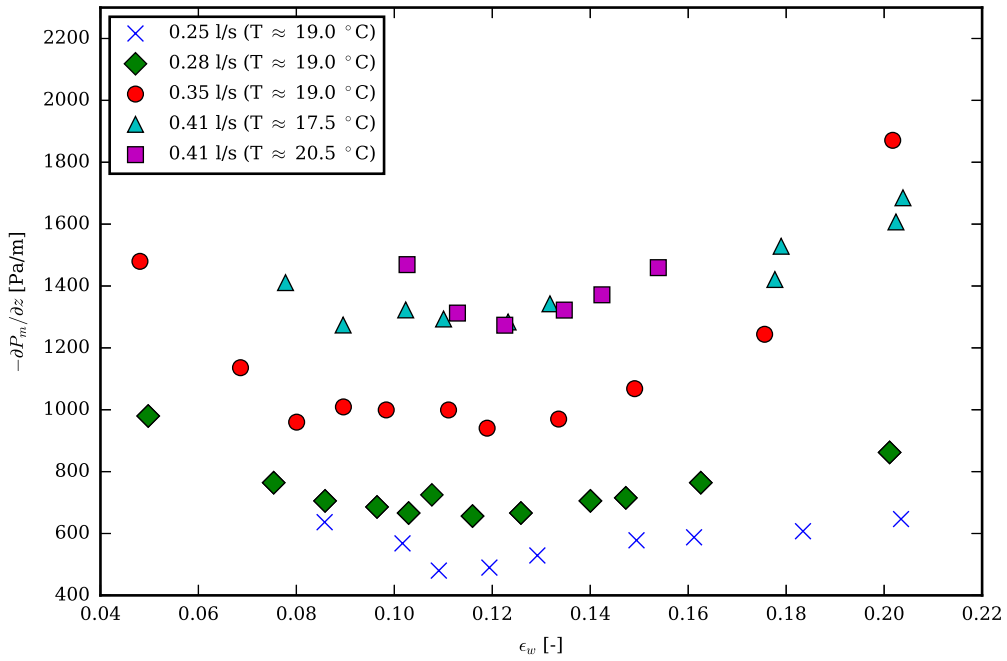

FIG. 5. Pressure drop as a function of the water addition ratio for all used values of the oil flow rate

II. NUMERICAL SIMULATIONS

A. Introduction

Full 3D and time-dependent numerical simulations have been carried out for some of our experiments. Important are the position and velocity of the core with respect to the pipe wall. Also the shape of the core-annular interface and the pressure build-up in the water annulus were investigated. The simulations were carried out without and with a turbulence model. These simulations can be regarded as an extension of those carried out by Ooms et al.[27], but now for horizontal core-annular flow with modelling of the turbulence in the water annulus. Similar numerical simulations (but without turbulence) have been carried out by Lee and Kang[21].

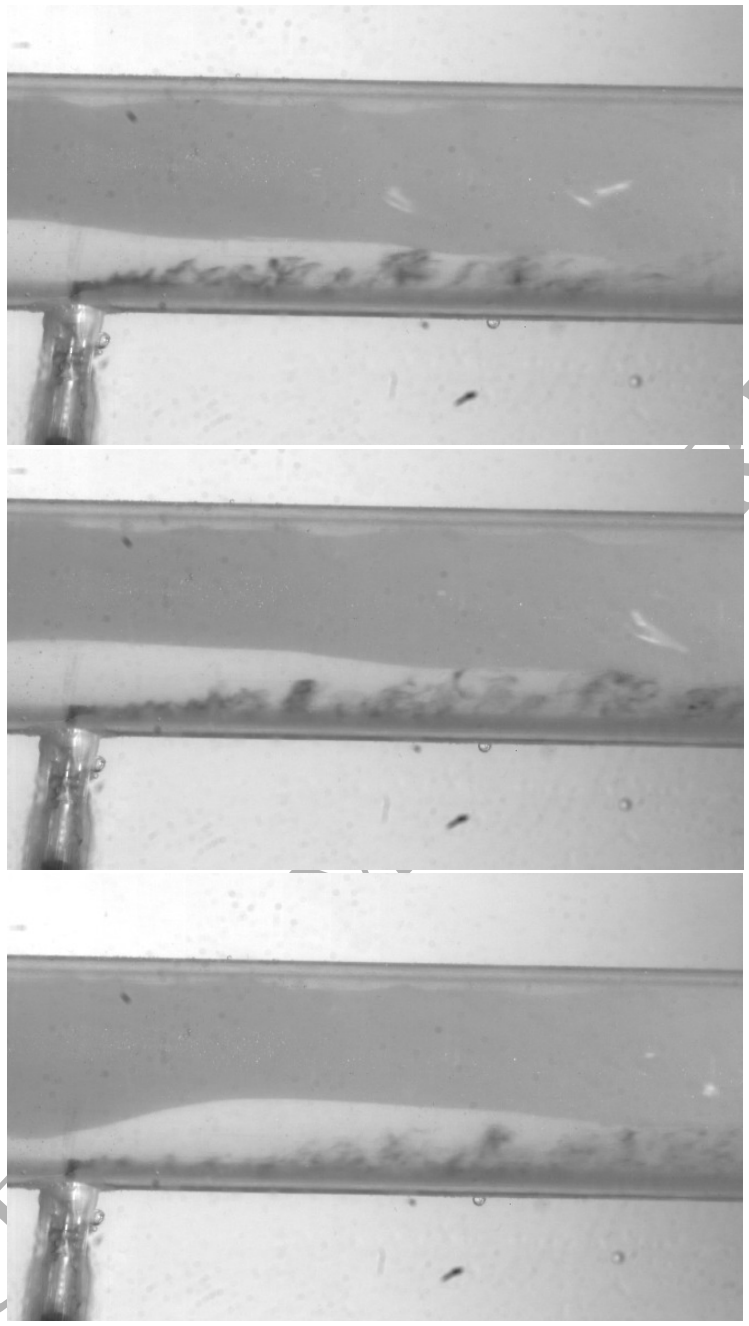

FIG. 6. Flow visualization of dye injected in the water layer at the bottom of the pipe. Top: directly after dye injection; middle: short time after the injection; bottom: the dye is leaving the field of view. Notice also the wave at the core-annular interface that moves to the right as a function of time.

B. Numerical scheme

The incompressible Navier-Stokes equations plus the mass conservation equation have been solved, with a density ρ and viscosity μ which are determined in each cell by the volume fraction of oil and water present. If the volume fraction of oil is α, and the density of oil is ρ_o and the density of water ρ_w, the density in a cell is $[\alpha\rho_o + (1-\alpha)\rho_w]$ and similarly for μ. The equations for both phases have been solved using the Finite Volume method, with application of the Volume of Fluid (VOF) method. This means that an advection equation is solved for the oil volume fraction α. The equations solved are as follows:

$$\rho = \alpha\rho_o + (1-\alpha)\rho_w \tag{1}$$

$$\mu = \alpha\mu_o + (1-\alpha)\mu_w \tag{2}$$

$$\frac{\partial \alpha}{\partial t} + \frac{\partial u_i \alpha}{\partial x_i} = 0 \tag{3}$$

$$\frac{\partial u_i}{\partial t} + u_j \frac{\partial u_i}{\partial x_j} = -\frac{1}{\rho}\frac{\partial p}{\partial x_i} + \nu \frac{\partial^2 u_i}{\partial x_j^2} + g_i + \frac{1}{\rho} s_i^* \tag{4}$$

$$\frac{\partial \rho u_i}{\partial x_i} = 0 \tag{5}$$

s_i^* is the interfacial tension term, which according to Brackbill et al.[6] is given by:

$$s_i^* = -\sigma^* \kappa \frac{\partial \alpha}{\partial x_i}\,, \tag{6}$$

in which σ^* is the interfacial tension and κ denotes the local interfacial curvature.

We used the package OpenFOAM (see[33]) for the simulations. Use was made of the interFoam solver, with backward Euler in time and a TVD scheme for the advection terms. The algorithm employs a compressive-flux model, which limits the diffusion of the indicator function. The pressure-velocity coupling was done using the PISO scheme. The following linear solvers have been used: Preconditioned Conjugate Gradient for the pressure, and Preconditioned Bi-Conjugate Gradient for velocity components. For stability reasons the Courant number was kept below 0.01 for all simulations. Such a low value of the Courant number is necessary to solve the very thin oil/water interface with the current method, as reported by Gopala and van Wachem[11]. The grids were block-structured with 125, 80, and 60 grid points in radial, circumferential and axial flow direction, respectively which

gives a total of approximately 500,000 grid points. In an earlier study (Ooms et al.[27]) we investigated the grid convergence and concluded that the number of grid points is sufficient. In axial direction the periodic boundary condition was imposed. At the pipe wall we prescribed the no-slip condition. As initial condition the analytical expression for concentric core-annular flow belonging to the relevant parameters (pipe radius, core radius, pressure drop, densities, viscosities and interfacial tension) was used (as in Beerens et al.[5]). During the calculation the imposed pressure gradient remained the same; this pressure gradient was applied via a body force.

A small-amplitude disturbance was assumed to be present at the core-annular interface at the start of the transient calculation. This stimulated the further growth of waves at the interface. The wavelength was chosen to be equal to the fastest growing wavelength found from linear stability calculations (see Joseph and Renardy[14]). The pipe length L was assumed to be equal to this wavelength. As for all simulations periodic boundary conditions were applied, an integer number of wavelengths had to fit in the calculation domain. (In an earlier study (see Beerens et al.[5]) we investigated numerically the development of the wavelength distribution in a much longer pipe for a vertical (axisymmetric), laminar core-annular flow. The average wavelength found in those simulations was close to the wavelength found from the linear stability theory.) As the core moved upward (in the present simulations for the horizontal pipe) as a function of time due to the buoyancy force, the thickness of the annular layer became small at the top of the pipe and rather large at the bottom. For that reason waves with a wavelength that is different from the initially imposed one could develop over time in the simulation and hence the number of wavelengths in the calculation domain could change. When a certain eccentricity is reached the upward movement of the core stops due to the levitation forces generated by the annular flow.

C. Numerical results

One experiment ($\epsilon_w = 15.1\,\%$, $Q_o = 0.35\,l/s$) has been studied in detail to assess the influence of turbulence in the water annulus. Much information will be given for that case. In addition two other experiments ($\epsilon_w = 9.65\,\%$, $Q_o = 0.28\,l/s$) and ($\epsilon_w = 20.1\,\%$, $Q_o = 0.28\,l/s$) were simulated for which less information is supplied here for the sake of brevity.

1. *Laminar simulation for experiment* ($\epsilon_w = 15.1\,\%$, $Q_o = 0.35\,l/s$)

For the first experiment we initially assumed that at the start of the calculation a concentric core-annular flow determined from the analytical solution was present, belonging to the following experimental parameters: the radius of the core and the pipe are respectively given by $R_1 = 9.4 \cdot 10^{-3}\,\mathrm{m}$ and $R_2 = 10.5 \cdot 10^{-3}\,\mathrm{m}$, the dynamic viscosities of the liquids in the core and annulus are $\mu_o = 2.318\,\mathrm{Pa\,s}$ and $\mu_w = 0.001\,\mathrm{Pa\,s}$, the densities are $\rho_o = 857\,\mathrm{kg/m^3}$ and $\rho_w = 1000\,kg/m^3$, the interfacial tension is $\sigma^* = 1.6 \cdot 10^{-2}\,N/m$ and the pressure gradient in the axial direction is $f^* = 1060\,\mathrm{Pa/m}$.

The core radius R_1 was calculated from the experimental oil and water flow rates using a correlation for the hold-up ratio h. h is defined as the ratio of the input oil-water flow rate ratio to the in-situ oil-water volume ratio (see also Li and Renardy[22]).

$$h = \frac{Q_o/Q_w}{V_o/V_w} = \frac{(1-\varepsilon_w)/\varepsilon_w}{\alpha/(1-\alpha)} \tag{7}$$

For concentric core-annular flow with a smooth interface the formula for h can be simplified. With $V_o = \pi R_1^2 L$ and $V_w = \pi(R_2^2 - R_1^2)L$:

$$h = \frac{Q_o/Q_w}{\left(\frac{\pi R_1^2 L}{\pi(R_2^2-R_1^2)L}\right)} = \frac{Q_o/Q_w}{\left(\frac{R_1^2}{R_2^2-R_1^2}\right)} = \frac{Q_o}{Q_w}\left(\frac{R_2^2}{R_1^2} - 1\right) \tag{8}$$

$$\Rightarrow \quad a = \frac{R_2}{R_1} = \sqrt{1 + h\frac{Q_w}{Q_o}} \tag{9}$$

Experiments by Bai et al.[2] show that the average value for the hold-up ratio $h = 1.39$ for vertical and horizontal core-annular flow, provided that the mixture velocity is reasonably high. In the remainder of this paper, it is assumed that the radius ratio a is related to the experimental flow rates via the hold-up ratio $h = 1.39$. R_1 is calculated via equation (9) and used here, although there is not a concentric and smooth core-annular flow but an eccentric disturbed core-annular flow.

The analytically calculated initial bulk oil velocity for concentric core-annular flow according to the above parameter values is significantly larger than the experimental value. The reason is that waves develop at the core-annular interface and that the core moves upward under the influence of buoyancy. The waves and eccentric core lead to a larger

stress at the oil-water interface, which slows down the oil. To numerically simulate this process takes a very long computation time. In the paper by Beerens et al.[5] it is suggested that starting from a bulk oil velocity for concentric core-annular flow already close to the experimental value (using the same pressure drop and core radius) speeds up the calculation considerably. We have, therefore, followed this approach in our simulations. It is important to realize that the final result of the (converged) simulation is independent of the chosen initial bulk oil velocity, if the pressure drop over the pipe and the core radius are the same for both cases. Of course, the initial bulk oil velocity will have an influence on the initial value of the hold-up ratio. However the final result will be the same.

First a laminar simulation was carried out and thereafter a turbulence model was applied. For the laminar case the position of the core as function of time is given in figure 7. As can be seen the core rises rather quickly, but never touches the wall (although it gets very close to it). To verify the convergence of the calculation we also calculated the upward momentum p_y of the entire core-annular flow (i.e. the core and annulus over the total pipe length) and the axial momentum p_z of the entire flow. The results are shown in figure 8. The upward momentum is still slightly increasing after 2.5 s, which means that the core is still moving upward very gradually (and hence the liquid in the annulus is flowing downward). As the core gets closer to the top part of the wall its flow resistance is increasing and therefore the axial momentum continues to decrease. The calculated mixture velocity has a value of $u_{mix} = 1.18\,m/s$, whereas the experimental one is equal to $1.10\,m/s$. (Note that the mixture velocity is equal to the ratio of the total throughput $(Q_o + Q_w)$ and the cross sectional area of the pipe.) In figure 9 the dimensionless axial velocity profile in the core and annulus (in a vertical cross-section through the centreline of the pipe) is given as a function of time. It has been made dimensionless by means of the calculated mixture velocity. There is a strong continuous increase in the annular velocity at the bottom of the pipe, which we did not observe during the flow visualization studies. The axial velocity becomes significantly larger than the experimental value. This increase in velocity at the bottom can also clearly be seen in a normal cross-section of the pipe (see figure 10). In this figure the velocity is given in m/s.

The conclusion is that the laminar flow simulation is not in agreement with the experi-

ment. As mentioned the flow visualization showed that turbulence can be expected in the water layer at the bottom of the pipe. Therefore the simulations were continued with the use of a turbulence model.

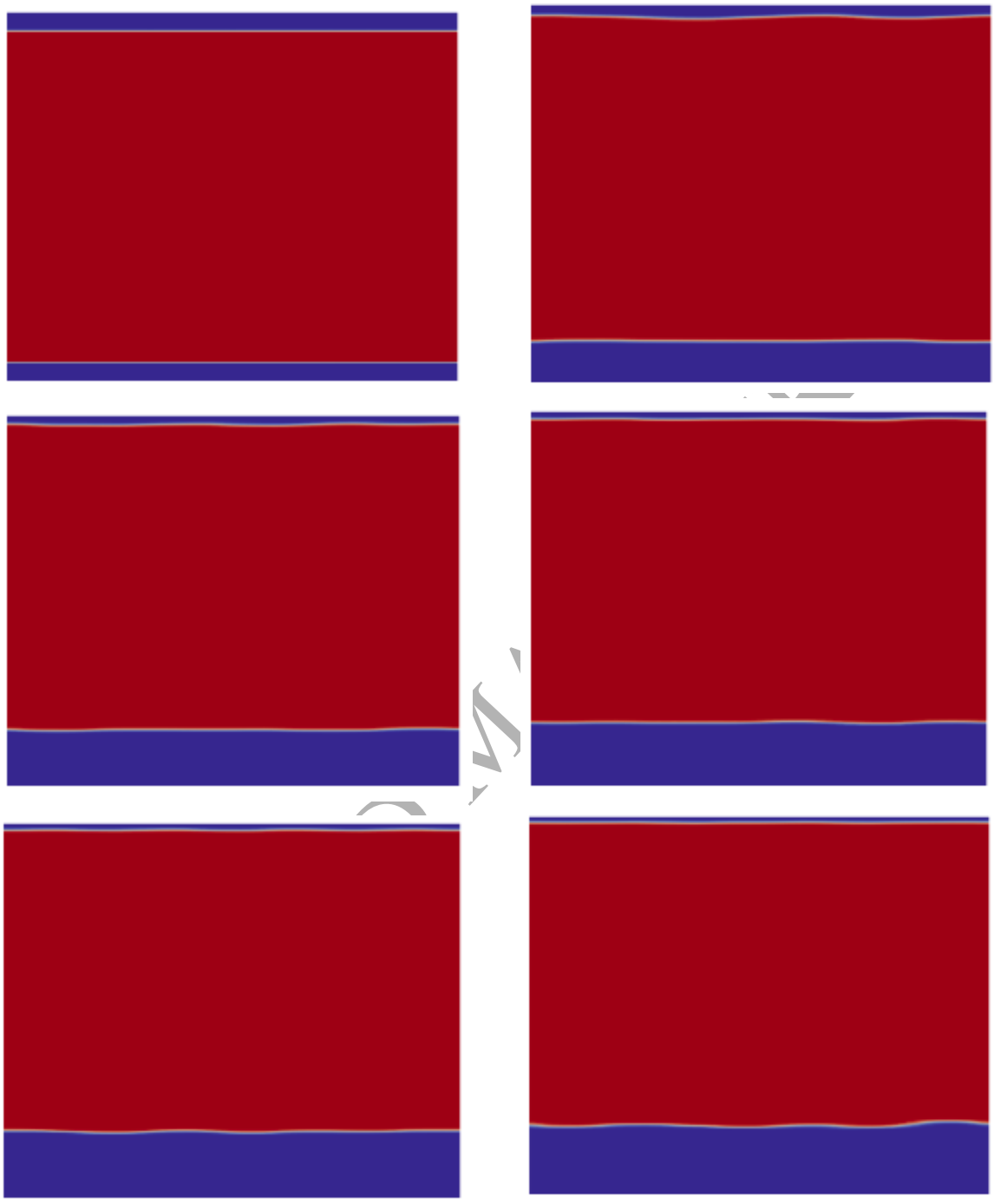

FIG. 7. Core position as a function of time in the laminar flow simulation. The simulation was started with an assumed concentric oil core at time zero. Top left: $t = 0.0\,s$; top right $t = 0.2\,s$; middle left: $t = 0.6\,s$; middle right $t = 1.2\,s$; bottom left: $t = 1.8\,s$; bottom right: $t = 2.354\,s$.

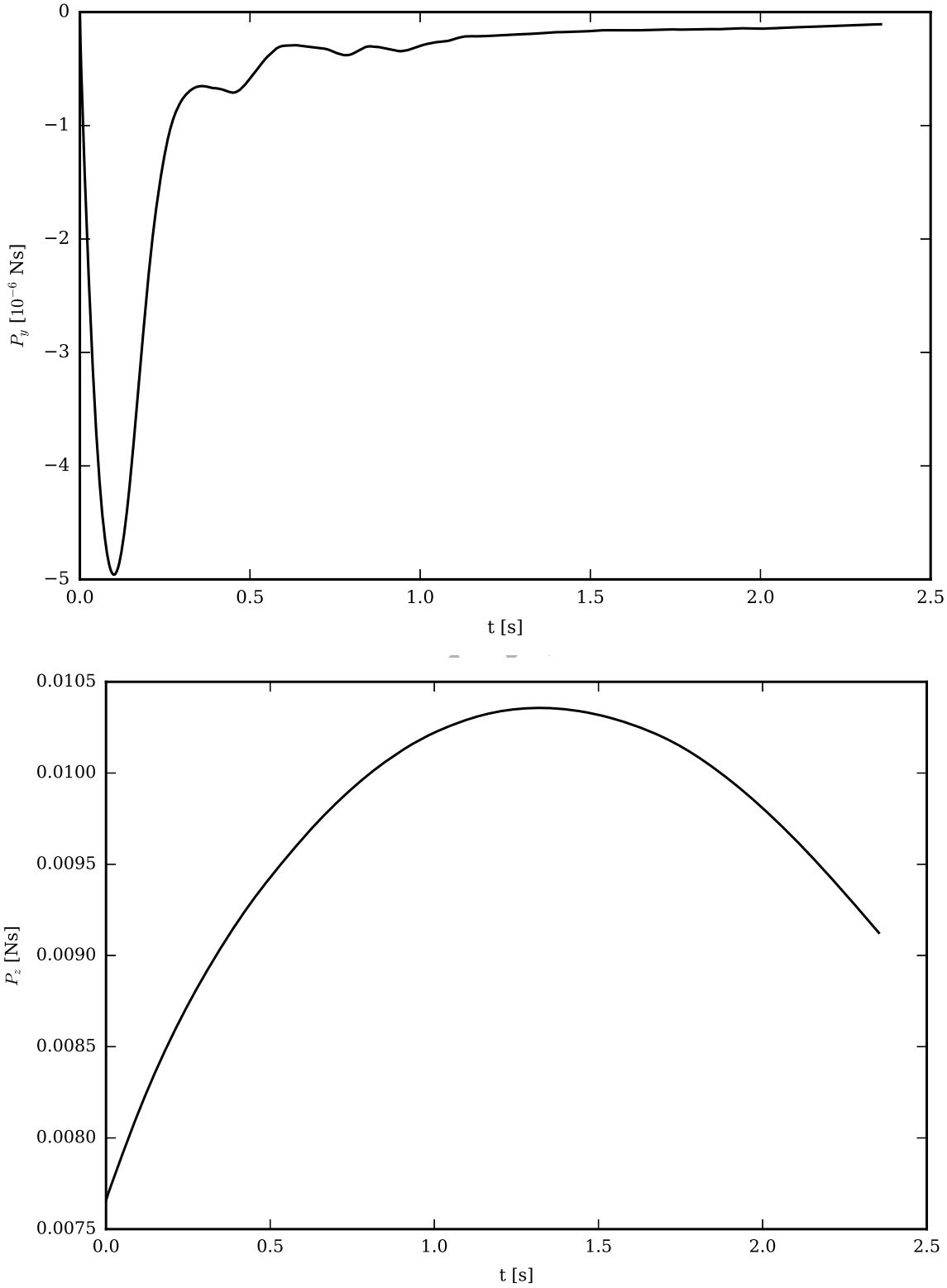

FIG. 8. Upward momentum and axial momentum of the total flow (core and annulus) as a function of time for the laminar simulation.

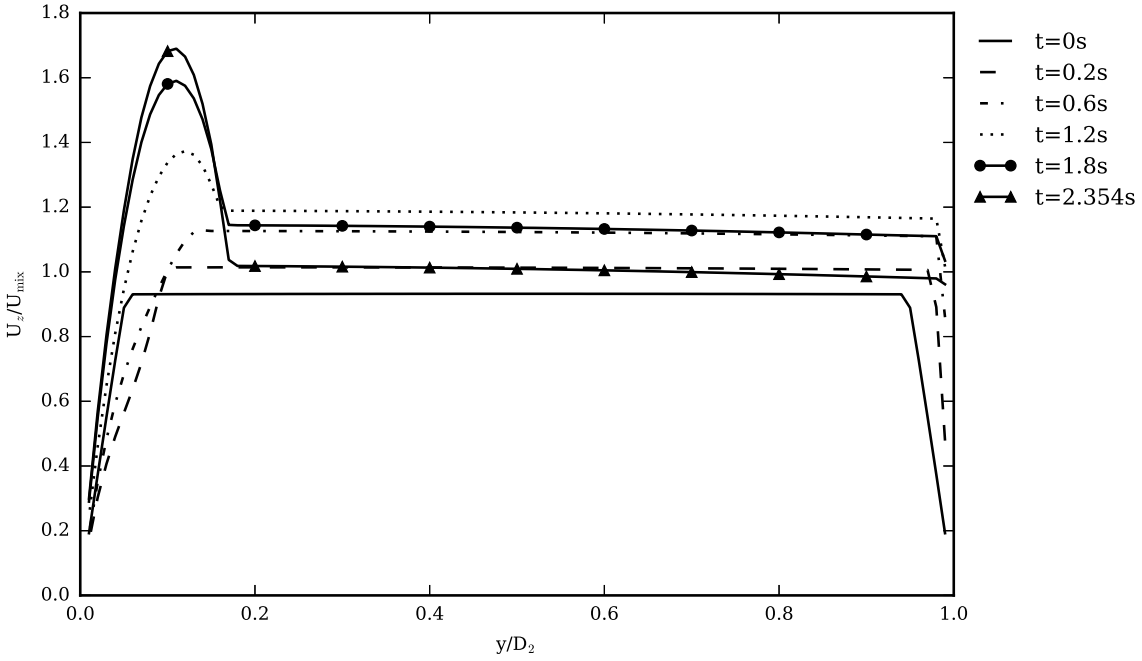

FIG. 9. Dimensionless axial velocity profile as a function of time for the laminar simulation. Left-hand side is bottom of the pipe; right-hand side the top of the pipe.

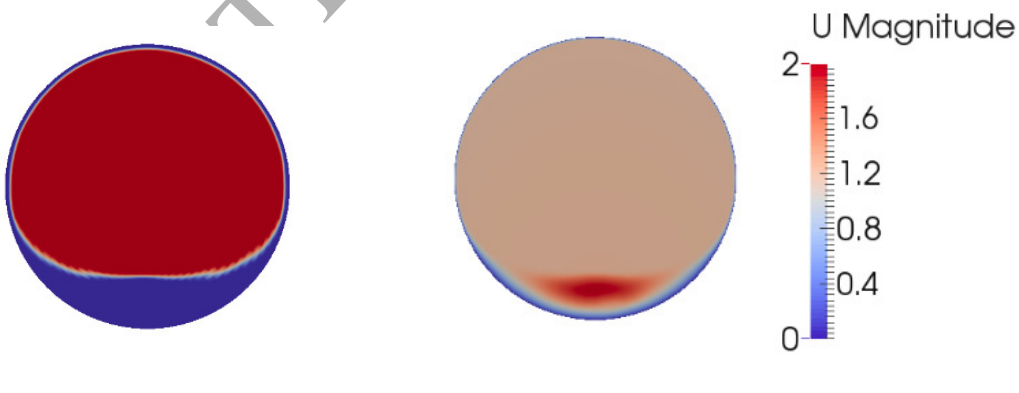

FIG. 10. Simulation for the laminar case. Left graph: core profile in a normal cross-section of the pipe (blue is water and red is oil). Right graph: axial velocity profile in a normal cross-section.The unit is m/s.

2. *Turbulent simulation for experiment* ($\epsilon_w = 15.1\,\%$, $Q_o = 0.35\,l/s$)

The low-Re Launder-Sharma $k-\varepsilon$ model has been used (see Launder and Sharma[20] for details). It has been applied to the same case as used for the laminar simulation discussed above. At the start of the simulation uniform internal turbulence properties were applied to the flow with $k_{int} = 0.2\,\mathrm{m}^2/\mathrm{s}^2$ and $\varepsilon_{int} = 200\,\mathrm{m}^2/\mathrm{s}^3$. The wall boundary conditions were $k_{wall} = 1.0 \cdot 10^{-15}\,\mathrm{m}^2/\mathrm{s}^2$ and $\varepsilon_{wall} = 1.0 \cdot 10^{-15}\,\mathrm{m}^2/\mathrm{s}^3$. The same pressure gradient and hold-up ratio were imposed as in the laminar simulation.

In figure 11 the position of the core is shown as a function of time. The simulation was (again) started with a concentric position of the core in the pipe. Just like in the laminar simulation the oil core moves to an eccentric position rather quickly. A significant difference, however, is that in the final situation the core is less eccentric than found in the laminar simulation. Furthermore, the waves at the upper and lower part of the interface have larger amplitudes. To investigate the time evolution in the simulation the upward momentum p_y of the entire core-annular flow and the axial momentum p_z of the entire flow were again calculated. The result is given in figure 12. It can be concluded that the flow reached an equilibrium state: p_z converges to a constant value and p_y fluctuates around an equilibrium value due to the passage of waves at the interface. The dimensionless axial velocity profile in the core and annulus (in a vertical cross-section through the centreline of the pipe) as a function of time is given in figure 13. It has been made dimensionless with the calculated mixture velocity, which has a value of $u_{mix} = 1.34\,m/s$ for this case. The peak in the water velocity at the bottom of the pipe (as found in the laminar calculation) is no longer present. This can also be concluded from figure 14, which shows the axial velocity in a normal cross-section of the pipe in m/s. The turbulent viscosity as a function of time is shown in figure 15. The model predicts that the turbulence viscosity in the water layer at the bottom part of the pipe is about 10 to 20 times larger than the water viscosity. The turbulence in the water at the top part of the pipe and the turbulence in the oil core (as assumed to be present at the start of the calculation) has damped out rather quickly. The reduced pressure distribution in the annulus is shown in figure 16. (The reduced pressure is defined as the pressure without the contribution due to gavity.) There is a pressure increase at the locations where the core gets too close to the pipe wall. These pressure variations

push the core from the pipe wall when it gets too close, making core-annular flow possible. Also reduced pressure contours are given in figure 17.

The calculated water addition ratio and oil flow rate are respectively $\epsilon_w = 16.0\,\%$ and $Q_o = 0.39\,l/s$, whereas the experimental values are slightly different, namely $\epsilon_w = 15.1\,\%$ and $Q_o = 0.35\,l/s$. This can be due to the physical modelling by means of the turbulence model and/or due the the application of the hold-up correlation ($h = 1.39$). The possible error due to the hold-up correlation could be avoided by keeping the flow rates of oil and water constant during the numerical simulation (and therefore also the water addition ratio and the mixture velocity) by adapting the value of R_1. Therefore instead of imposing the the pressure drop and hold-up ratio in the simulation (which gives the water and oil flow rates as output), the water and oil flow rates can be imposed (which gives the pressure drop and hold-up ratio as output). The latter approach was used by Kouris and Tsamopoulos[19]. Another possibility to check the reliability of the numerical simulation against experiments is by first carrying out a numerical simulation for a certain case with given pressure drop and hold-up ratio, calculating the values of ϵ_w and Q_o as output parameters for this case, and thereafter performing an experiment for these flow rate values and compare the measured pressure drop and holdup ratio with the ones used for the simulation. In this way the hold-up correlation is not required and possible differences between the experimental and numerical pressure drop are only due to the physical modelling of the flow. We have followed this approach for the present case. Starting from the calculated flow rates of oil and water ($\epsilon_w = 16.0\,\%$ and $Q_o = 0.39\,l/s$) we have determined the measured pressure drop for this case by interpolating the data in figure 5 and found $\sim 1250\,Pa/m$. This is about 15 % larger than the numerical value. We will come back to this in the discussion.

The calculated hold-up ratio as a function of time is given in figure 18. The flow rates were taken at the entrance to the pipe. The fluctuations are due to the passage of waves through the pipe. The initial high value is due to using at the start of the simulation a bulk oil velocity for concentric core-annular flow already close to the experimental value (as discussed).

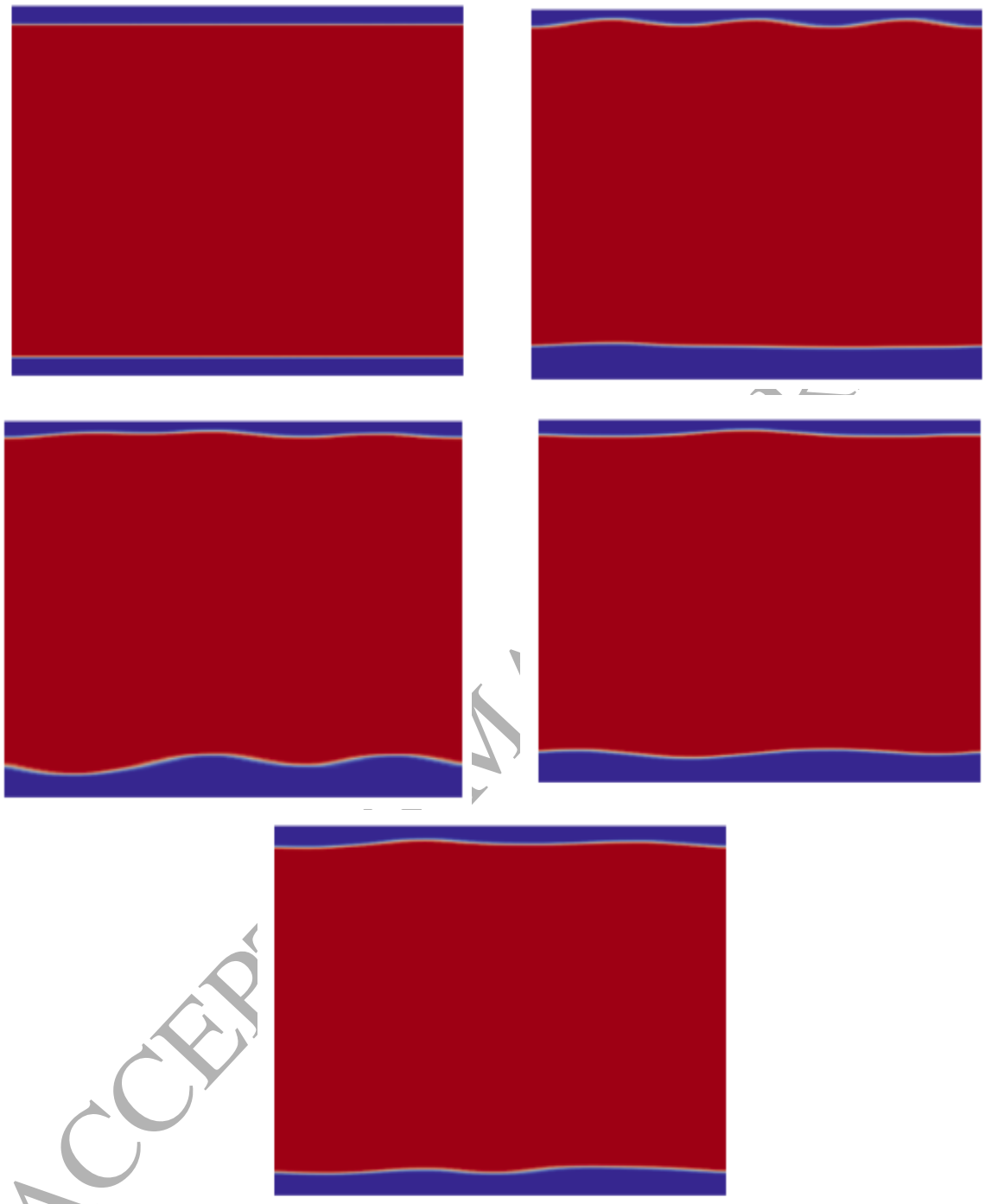

FIG. 11. Core position as a function of time in the turbulent simulation with the Launder-Sharma model. The simulation was started with an assumed concentric core. Top left: $t = 0.0\,s$; top right: $t = 0.2\,s$; middle left: $t = 0.6\,s$; middle right: $t = 1.2\,s$; bottom: $t = 1.52\,s$.

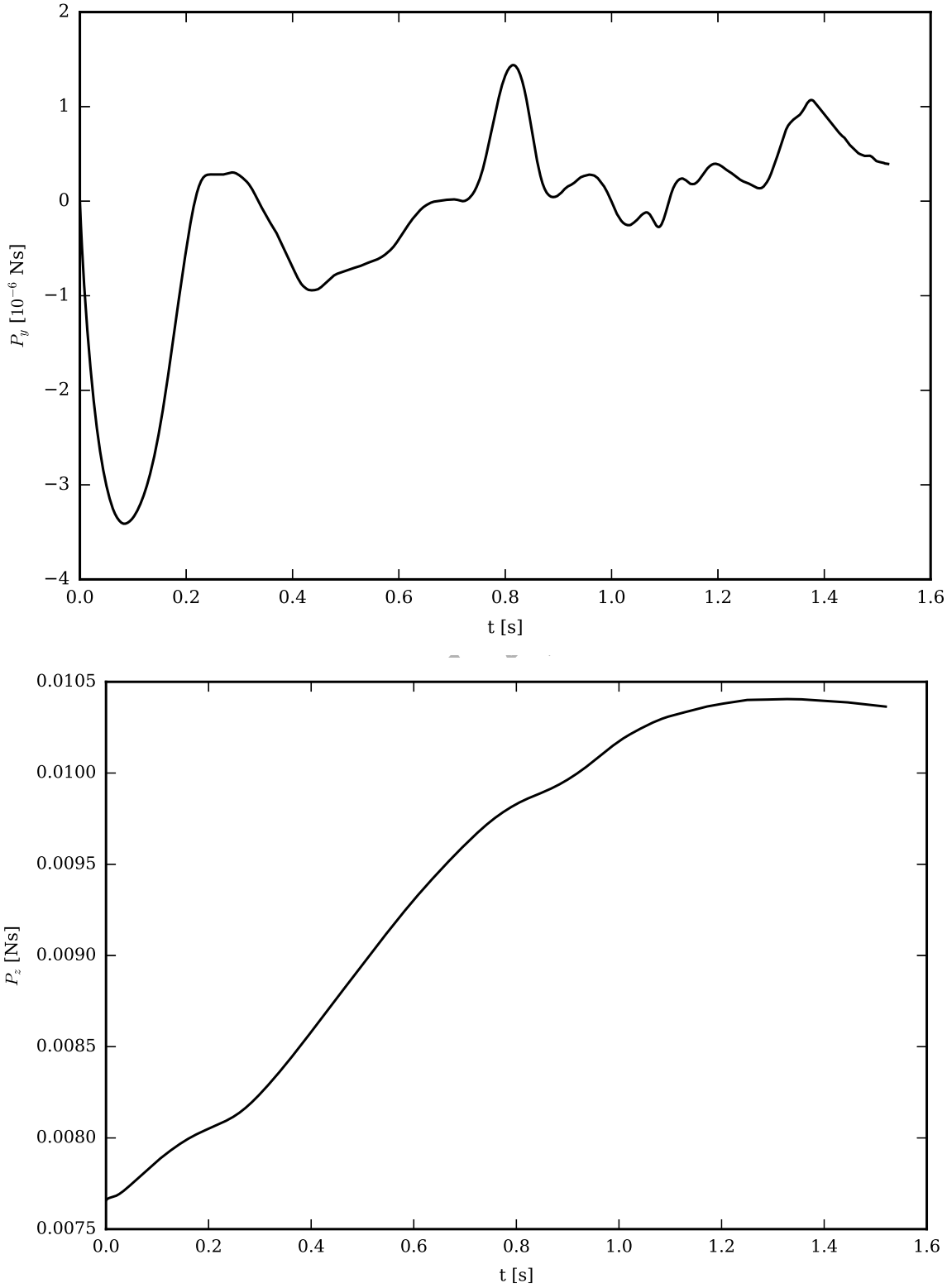

FIG. 12. Upward and axial momentum of the core as a function of time in the turbulent simulation with the Launder-Sharma model.

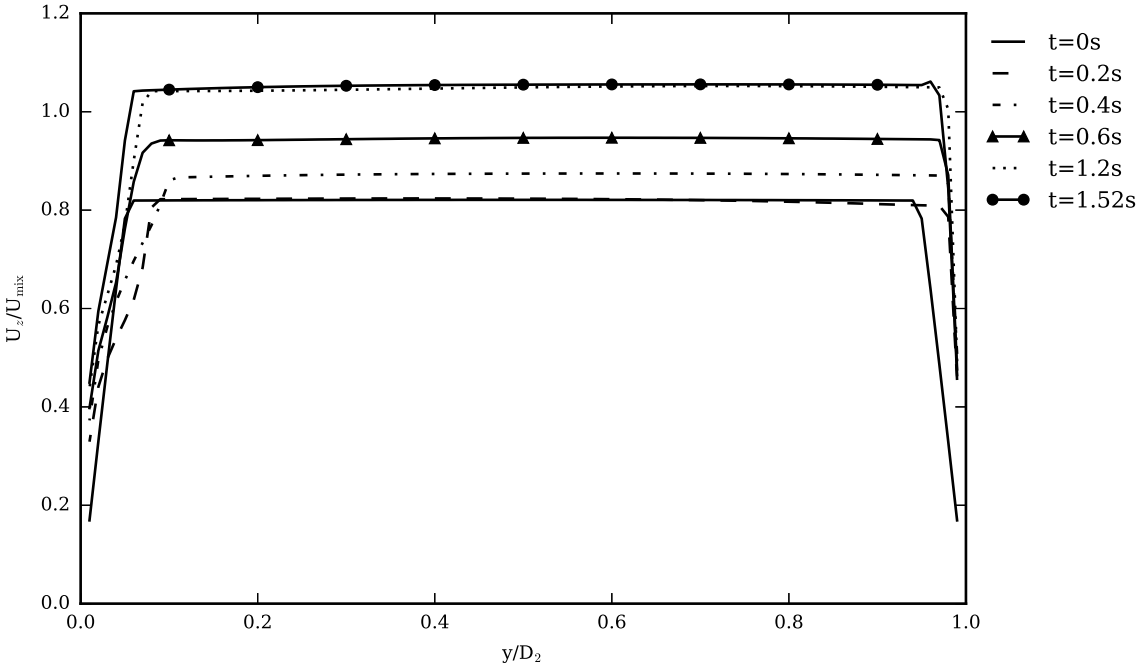

FIG. 13. Axial velocity profile as a function of time in the turbulent simulation with the Launder-Sharma model. Left-hand side is bottom of the pipe; right-hand side the top of the pipe.

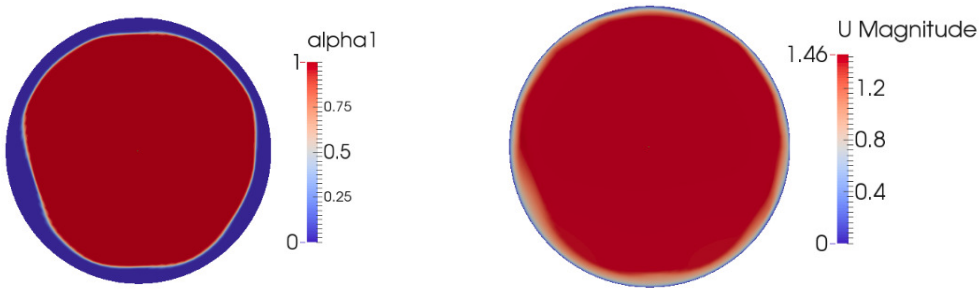

FIG. 14. Turbulent simulation with the Launder-Sharma model. Left graph: core profile in a normal cross-section of the pipe (blue is water and red is oil). Right graph: axial velocity profile in a normal cross-section. The unit is m/s.

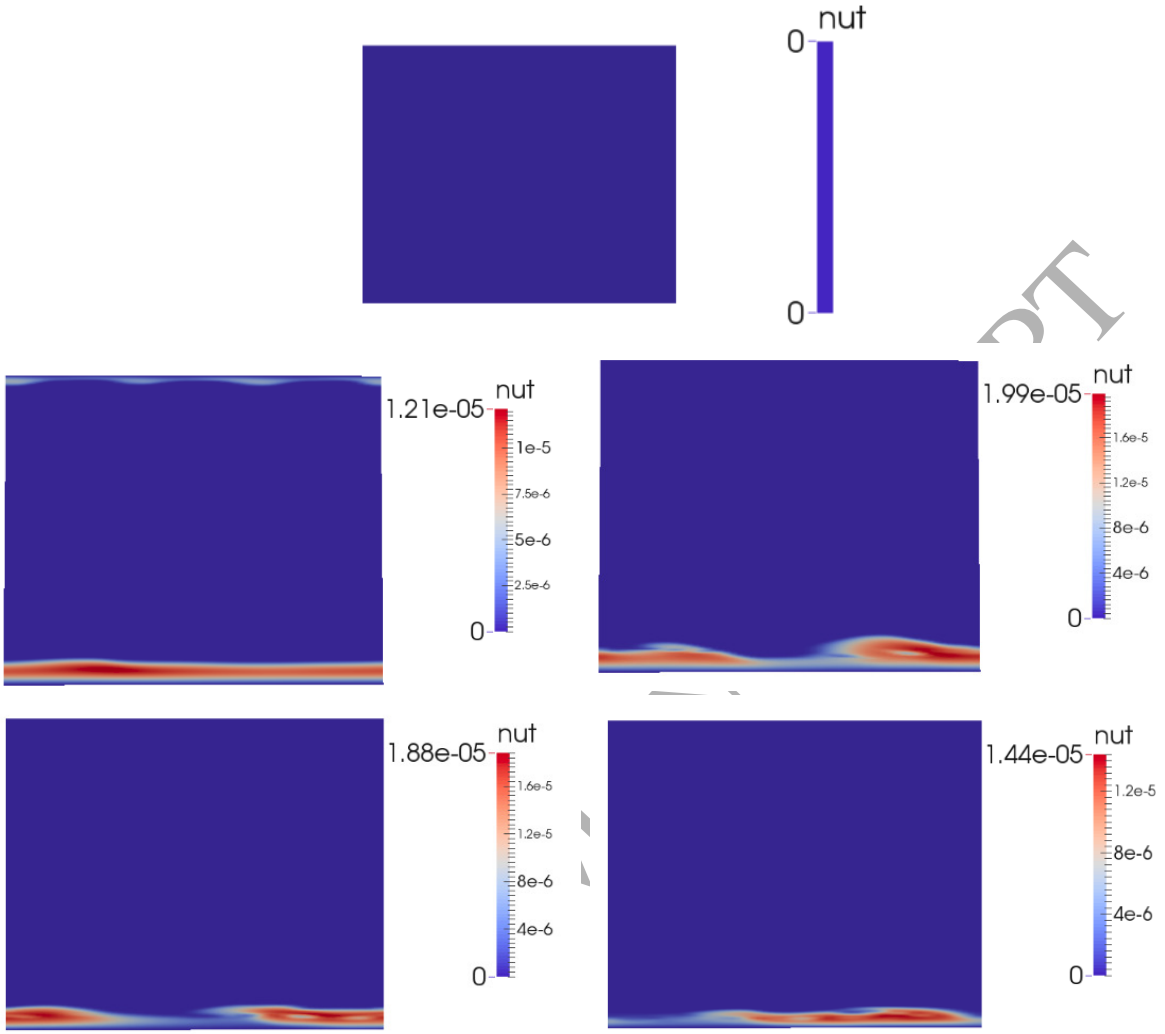

FIG. 15. Turbulent viscosity as a function of time in the turbulent simulation with the Launder-Sharma model. Top : $t = 0.0\,s$; middle left: $t = 0.2\,s$; middle right: $t = 0.6\,s$; bottom left: $t = 1.2\,s$ bottom right: $t = 1.52\,s$. It can be seen that the flow is only turbulent in the water layer at the bottom of the pipe. The value of the turbulent viscosity changes with the thickness of the annular layer due the movement of the wave at the interface. The unit is m^2/s.

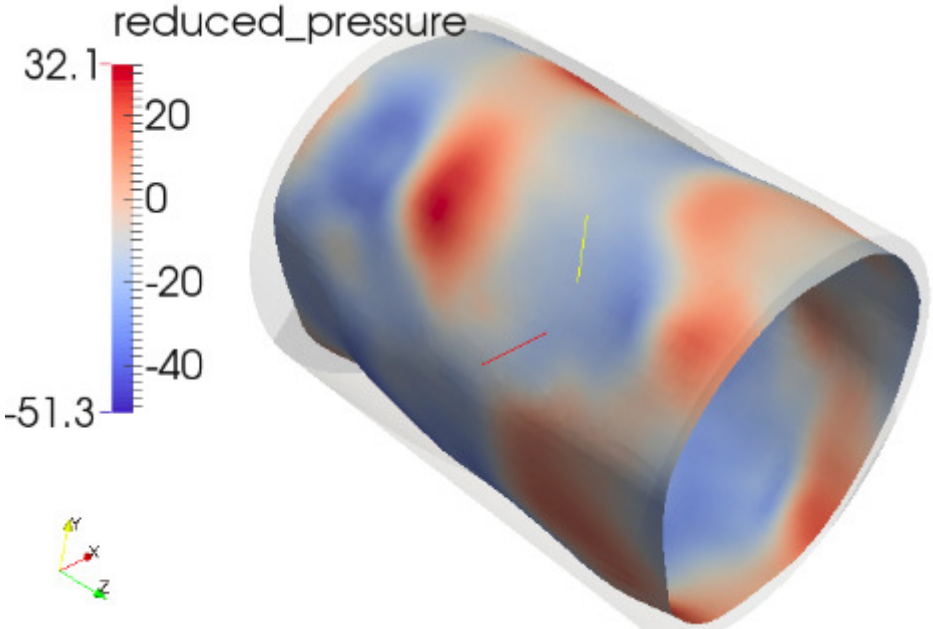

FIG. 16. 3D profile of the reduced pressure at the core-annular interface in the turbulent simulation with the Launder-Sharma model. The unit is Pa.

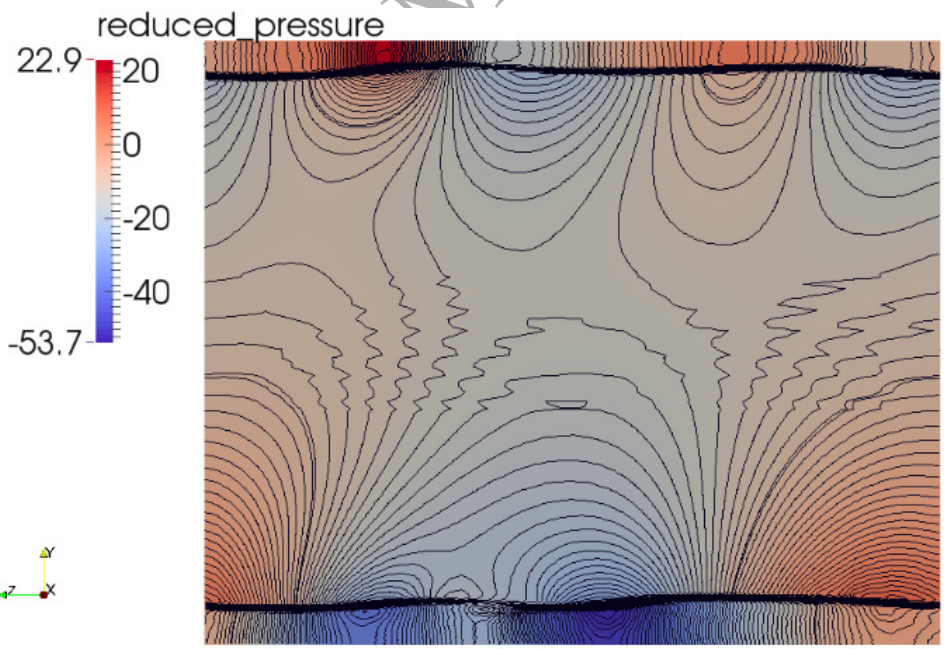

FIG. 17. Reduced pressure contours in the turbulent simulation with the Launder-Sharma model. The unit is Pa.

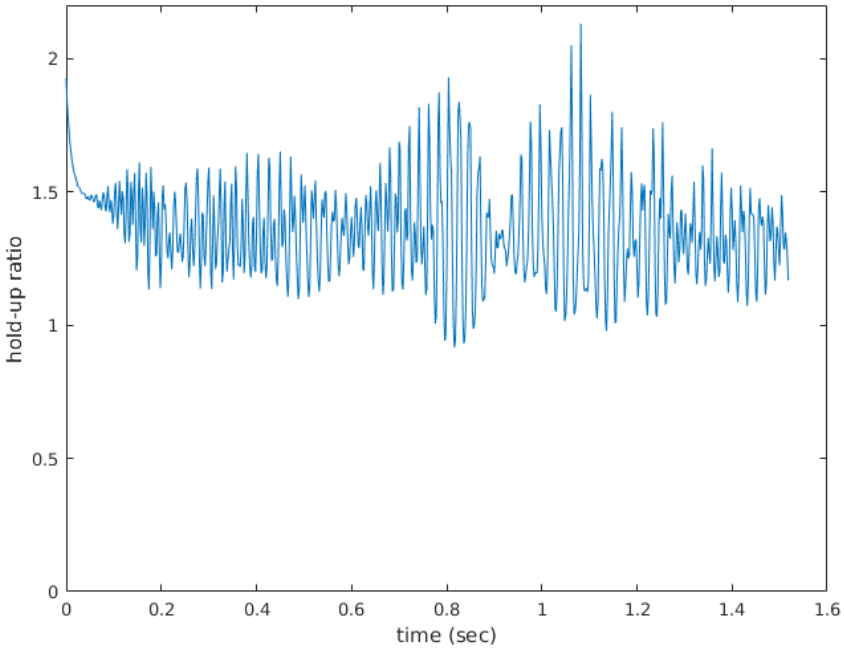

FIG. 18. Hold-up ratio as a function of time

3. Turbulent simulation for experiments ($\epsilon_w = 9.65\,\%$, $Q_o = 0.28\,l/s$) and ($\epsilon_w = 20.1\,\%$, $Q_o = 0.28\,l/s$)

Two more experiments ($\epsilon_w = 9.65\,\%$, $Q_o = 0.28\,l/s$ and $\epsilon_w = 20.1\,\%$, $Q_o = 0.28\,l/s$) have been simulated using the Launder-Sharma model. The experimental and numerical values of the mixture velocities are given in table I. The conclusions from the results of

$u_{mix}\ (m/s)$	**Experimental**	**Numerical**
$\epsilon_w = 9.65\,\%$, $Q_o = 0.28\,l/s$	0.893	0.973
$\epsilon_w = 20.1\,\%$, $Q_o = 0.28\,l/s$	1.01	1.26

TABLE I. Comparison of the experimental and numerical mixture velocities.

these simulations are similar to those for experiment ($\epsilon_w = 15.1\,\%$, $Q_o = 0.35\,l/s$). So for the sake of brevity we leave out these detailed results.

High-speed movies were made of these experiments. In figure 19 and figure 20 the experimental observation and their numerical simulation are shown. We calculated the wavelengths and amplitudes for the interfacial waves. The distance in axial direction between two tops in the wave was defined as 'wavelength'. This procedure explains why there are multiple values for the wavelength. Half the distance in vertical direction between the crest (the top) and the trough of the wave is defined as amplitude. The results for the two figures are given in table II and table III. The predicted wavelengths shows reasonably good agreement with the experimental ones. The wave amplitude at the top of the pipe is underpredicted, whereas at the bottom the agreement is better.

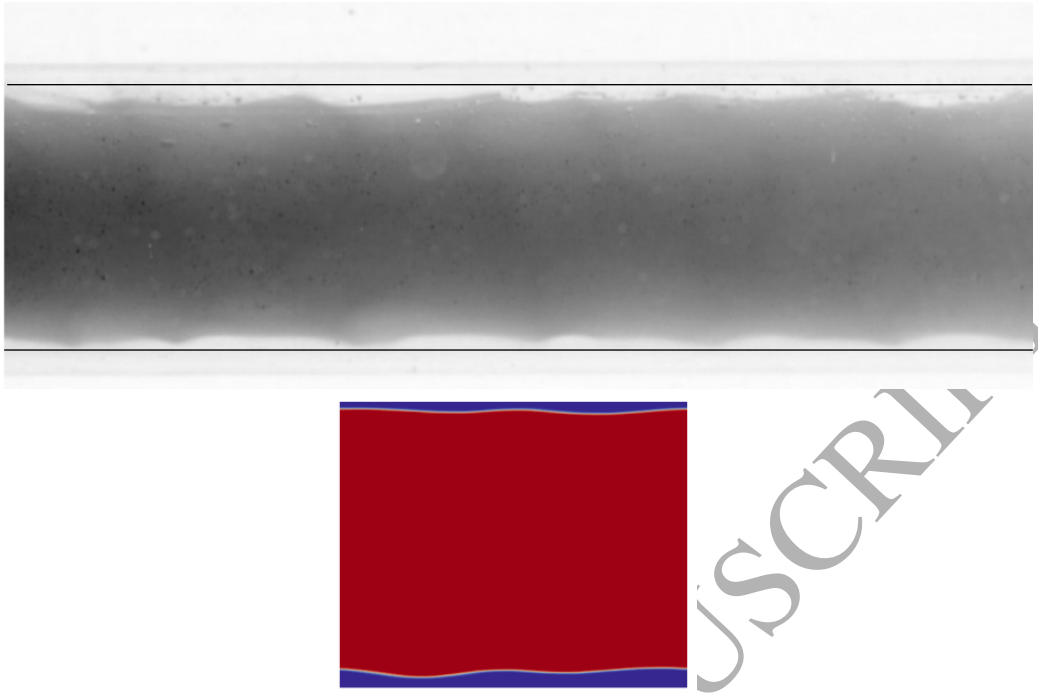

FIG. 19. Experiment and (converged) simulation for experiment ($\epsilon_w = 9.65\,\%$, $Q_o = 0.28\,l/s$). The solid lines indicate the pipe wall.

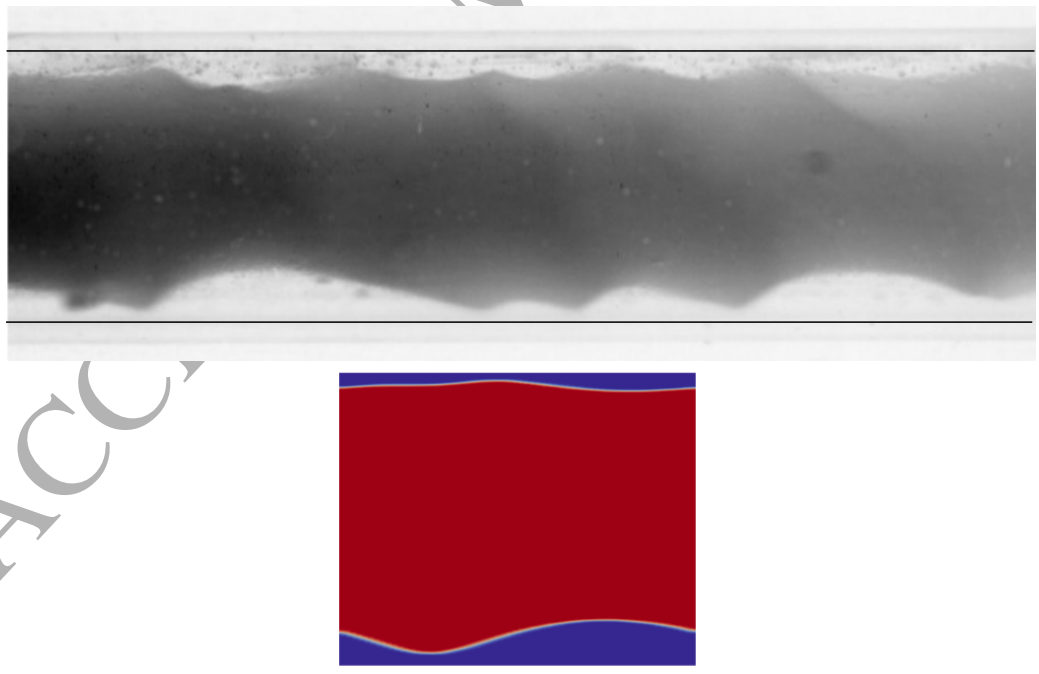

FIG. 20. Experiment and (converged) simulation for experiment ($\epsilon_w = 20.1\,\%$, $Q_o = 0.28\,l/s$). The solid lines indicate the pipe wall.

Parameter	**Numerical**	**Experimental**
Amplitude	Upper Annulus	Upper Annulus
	0.02	0.06
	0.02	0.05
		0.05
		0.04
	Lower Annulus	Lower Annulus
	0.03	0.07
	0.02	0.04
		0.05
		0.04
Wavelength	Upper Annulus	Upper Annulus
	1.31	1.35
	1.20	1.55
		1.45
		1.25
	Lower Annulus	Lower Annulus
	1.35	1.43
	1.15	1.34
		1.47
		1.40

TABLE II. Comparison of the experimental and numerical amplitudes and wavelengths belonging to figure 19. The unit of all quantities is cm.

Parameter	**Numerical**	**Experimental**
Amplitude	Upper Annulus	Upper Annulus
	0.04	0.09
	0.03	0.08
		0.07
		0.07
		0.07
	Lower Annulus	Lower Annulus
	0.12	0.15
		0.03
		0.09
		0.12
Wavelength	Upper Annulus	Upper Annulus
	0.91	1.47
	1.59	1.11
		0.91
		1.21
		1.78
	Lower Annulus	Lower Annulus
	2.52	2.68
		0.72
		1.25
		2.13

TABLE III. Comparison of the experimental and numerical amplitude and wavelengths belonging to figure 20. The unit of all quantities is cm.

III. CONCLUSION

Simulating core-annular flow by solving the Navier-Stokes equations is rather complex. The solution based on perfect core-annular flow with a concentric and smooth interface is usually not accurate enough for most applications. The reason is that waves are present at the interface and (in case of horizontal core-annular flow) that the core has an eccentric position in the pipe due to the buoyancy force on the core caused by the density difference between the core liquid and annular liquid. The incorporation of the waves and the eccentricity in the calculation is crucial for simulating the levitation force that keeps the core free from the pipe wall and for simulating the flow properties. In the present work it was shown that with nowadays numerical techniques and computer power it has become possible to simulate wavy and eccentric core-annular flow by solving the Navier-Stokes equation while taking the influence of turbulence in the annulus into account. The agreement with experiments in vertical flow (see Beerens et al.[5]) and horizontal flow (the present work) is encouraging. However, significant improvements are still possible. The difference between the experimental pressure drop and the numerically predicted one for given flow rates of oil and water can be of the order of 15 %. Also the predicted wave amplitude is significantly smaller than the measured one (in particular at the top of the pipe).

In this paper special attention has been given to the occurrence of trubulence in the annulus. The use of the low-Re Launder-Sharma $k-\varepsilon$ model significantly improved the comparison between the simulation results and the experiments, when compared to the simulation case without turbulence. The SST $k-\omega$ model has also been applied. The results for the SST $k-\omega$ are almost the same as for the Launder-Sharma $k-\varepsilon$ model and for the sake of brevity left out of this paper. Perhaps the use of a large eddy simulation can lead to an even better agreement between the predictions and the experiments.

ACKNOWLEDGMENT

The authors are grateful to Edwin Overmars and Carsten Sanders from the Laboratory for Aero- & Hydrodynamics for their support in making flow visualizations by means of high-speed movies.

REFERENCES

[1]Arney, M.S., Bai, R., Guevara, E., Joseph, D.D., Liu, K., 1993. Friction factor and hold-up studies for lubricated pipelining -I, Int. J. Multiphase Flow **19**,no.6, 1061-1076.

[2]Bai, R., Chen, K., Joseph, D.D., 1992. Lubricated pipelining: stability of core-annular flow. Part 5. Experiments and comparison with theory, J. Fluid Mech. **240**, 97-142.

[3]Bai, R., Kelkar, K., Joseph, D.D., 1996. Direct simulation of interfacial waves in a high-viscosity-ratio and axisymmetric core-annular flow, J. Fluid Mech. **327**, 1-34.

[4]Bannwart, A.C., 2001. Modeling aspects of oil-water core-annular flows, J. Petroleum Science and Engineering **32**, 127-143.

[5]Beerens, J.C., Ooms, G., Pourquie, M.J.B.M. 2014. A comparison between numerical predictions and theoretical and experimental results for laminar core-annular flow, AIChE J **60**, 3046-3056.

[6]Brackbill, J.U., Kothe, D.B., Zemach, C., 1992. A continuum method for modeling surface tension, Journal of Computational Physics **100**, 335-354.

[7]Brauner, N., Moalem Maron, D., 1992. Flow pattern transitions in two-phase liquid-liquid flow in horizontal pipes, Int. J. Multiphase Flow **18** No.1, 123-140.

[8]Charles, M.E., Govier, G.W., Hodgson, G.W., 1961. The horizontal pipeline flow of equal density oil-water mixtures, Can. J. Chem. Engng. **39**, 27-36..

[9]Colombo, L.P.M., Guillizzoni, M., Sotgia, G.M., 2012. Characterization of the critical transition from annular to wavy-stratified flow for oil-water mixtures in horizontal pipes, Exp. Fluids **53**, 1617-1625.

[10]Ghosh, S., Das, G., Das, P.K., 2010. Simulation of core annular downflow through CFD-A comprehensive study, Chemical Engineering and Processing **49**, 1222-1228.

[11]Gopala, V.R., van Wachem, B,G.M., 2008. Volume of fluid methods for immiscible-fluid and free-surface flows, Chemical Engineering Journal, **141** (1-3), 204-221.

[12]Huang, A., Christodoulou, C., Joseph, D.D., 1994. Friction factor and hold-up studies for lubricated pipelining-II; Laminar and $k-\varepsilon$ models for eccentric core flow, Int. J. Multiphase Flow **20**(no. 3), 481-491.

[13]Jiang, F., Wang, Y., Ou, J., Xiao, Z., 2014. Numerical simulation on oil-water annular flow through the II bend, Ind. Eng. Chem. Res. **53**, 8235-8244.

[14]Joseph, D.D., Renardy,Y.Y., 1993. Fundamentals of two-fluid dynamics, part II: Lubricated transport, drops and miscible liquids, Springer-Verlag, New York.

[15]Joseph, D.D., Bai, D., Chen K.P., Renardy, Y.Y., 1999. Core-annular flows, Ann. Rev. Fluid Mech. **29**, 65-90.

[16]Kaushik, V.V.R., Ghosh, S., Das, G., Das, P.K., 2012. CFD simulation of core-annular flow through sudden contraction and expansion, Journal of Petroleum Science and Technology **86-87**, 153-164.

[17]Kim, K., Choi, H., 2015. Characteristics of turbulent core-annular flow in a vertical pipe, International Symposium on turbulence and shear flow June 30 - July 5, Melbourne, Australia. Proceedings 1A-5.

[18]Ko, T., Choi, H.G., Bai, R., Joseph, D.D., 2002. Finite element method simulation of turbulent wavy core-annular flows using a $k-\omega$ turbulence model method, Int. J. Multiphase Flow **28**, 1205-1222.

[19]Kouris, C., Tsamopoulos, J., 2001. Dynamics of axisymmetric core-annular flow in a straight pipe. I. The more viscous fluid in the core, bamboo waves, Phys. Fluids **13** (no. 4), 841-853.

[20]Launder, B.E., Sharma, B.I. 1974. Application of the energy dissipation model of turbulence to the calculation of flow near a spinning disc, Letters in Heat and Mass Transfer **1**, (no. 2), 131-137.

[21]Lee, B., Kang, M., 2016. Full 3D simulations of two-phase core-annular flow in horizontal pipe using level set method, J.Sci.Computing **66**, 1025-1051.

[22]Li, J., Renardy, Y.Y., 1999. Direct simulation of unsteady axisymmetric core-annular flow with high viscosity ratio, J. Fluid Mech. **391**, 123-149.

[23]Miesen, R., Beijnon, G., Duijvestijn, P.E.M., Oliemans, R.V.A., Verheggen, T., 1992. Interfacial waves in core-annular flow J. Fluid Mech. **238**, 97-117.

[24]Oliemans, R.V.A., Ooms, G.,1986. Core-annular flow of oil and water through a pipeline, Multiphase Science and Technology (ed. G.F. Hewitt, J.M. Delhaye and N. Zuber), vol. 2, Hemisphere, Washington, 427-476.

[25]Oliemans, R.V.A., Ooms, G., Wu, H.L., Dijvestijn, A., 1987. Core-annular oil/water flow: The turbulent-lubricating-film model and measurements in 5 cm pipe loop, Int. J. Multiphase Flow **13** no 1, 23-31.

[26]Ooms, G., 1972. The hydrodynamic stability of core-annular flow of two ideal liquids, Appl. Sci. Res. **26**, 147-158.

[27]Ooms, G., Pourquie, M.J.B.M., Beerens, J.C. 2013. On the levitation force in horizontal core-annular flow with a large viscosity ratio and small density ratio, Phys. Fluids **25**, 032102, 1-16.

[28]Renardy, Y.Y., 1997. Snakes and corkscrews in core-annular down-flow of two liquids, J. Fluid Mech. **340**, 297-317.

[29]Rodriguez, O.M.H., Bannwart, A.C., 2006. Experimental study on interfacial waves in vertical core-annular flow, J. Petroleum Science and Engineering, **54**, 140-148.

[30]Rodriguez, O.H.M., Bannwart, A.C., 2008. Stability analysis of core-annular flow and neutral stability wave number, AIChE J. **54** No.1, 20-31.

[31]Sotgia, G.M., Tartarini, P., Stalio, E., 2008. Experimental analysis of flow regimes and pressure drop reduction in oil-water mixtures, Int. J. Multiphase Flow **34**, 1161-1174.

[32]Strazza, D., Grassi, B., Demori, M., Ferreri, V., Poesio, P.,2012. Core-annular flow in horizontal and slightly inclined pipes: existence, pressure drops, and hold-up, Chem. Eng. Sci. **66**, 2853-2863.

[33]The OpenFOAM open source toolbox is produced by ESI-OpenCFD and is distributed through the OpenFOAM Foundation. OpenCFD was founded by Henry Weller, Chris Greenshields, and Mattijs Janssens.

[34]Ullmann, A., Brauner, N., 2004. Closure relations for the shear stress in two-fluid models for core-annular flow, Multiphase Science and Technology **16**, 355-397.